Journal of Power Sources 185 (2008) 466–472

Contents lists available at ScienceDirect

Journal of Power Sources

journal homepage: www.elsevier.com/locate/jpowsour

Effects of TiO_2 coating on high-temperature cycle performance of $LiFePO_4$-based lithium-ion batteries

Hao-Hsun Chang[a], Chun-Chih Chang[a], Ching-Yi Su[b], Hung-Chun Wu[b], Mo-Hua Yang[b], Nae-Lih Wu[a,*]

[a] Department of Chemical Engineering, National Taiwan University, Taipei 106, Taiwan, ROC
[b] Material and Chemical Research Laboratories, Industrial Technology Research Institute, Chutung, Hsinchu 310, Taiwan, ROC

ARTICLE INFO

Article history:
Received 20 March 2008
Received in revised form 3 July 2008
Accepted 11 July 2008
Available online 22 July 2008

Keywords:
Lithium-ion batteries
$LiFePO_4$
Capacity fading
TiO_2
Coating

ABSTRACT

$LiFePO_4$ particles were coated with TiO_2 (molar ratio = 3%) via a sol–gel process, and the effects of the coating on cycle performance of $LiFePO_4$ cathode at 55 °C against either a Li or a C (mesocarbon microbead) anode were investigated. It was found that, while the coating reduces capacity fading of the $LiFePO_4$/Li cell, it imposes a deteriorating effect on the $LiFePO_4$/C cell. Analyses on cell impedance and electrode surface morphology and composition showed that the oxide coating reduced Fe dissolution from the $LiFePO_4$ cathode and hence alleviated the impedance increase associated with the erosion process. This leads to reduced capacity fading as observed for the $LiFePO_4$/Li cell. However, the oxide coating itself was eroded upon cycling, and the dissolved Ti ions were subsequently reduced at the anode surface. Ti deposit on the C anode was found to be more active than Fe in catalyzing the formation of the solid-electrolyte interphase (SEI) layer, causing accelerated capacity decay for the $LiFePO_4$/C cell. The results point out the importance of evaluating the effect of cathode coating material on the anode side, which has generally been overlooked in the past studies.

1. Introduction

Lithium-ion secondary batteries have extensively been applied in electronic devices. $LiCoO_2$ is by far the most successful commercial cathode material. However, there has been constant effort made to find cheaper, less toxic, and more available cathode materials to replace the Co-based ones. $LiFePO_4$ [1] was firstly demonstrated by Padhi et al. [2] as a potential cathode material for Li-ion secondary batteries, and it has lately drawn considerable attention not only for its properties matching the needs mentioned above but also for its high safety and theoretical capacity (170 mAh g^{-1}). $LiFePO_4$ has the drawback of poor electronic conductivity, and mainly two methods have been adopted to circumvent this drawback, including carbon coating [3–5] and cation doping [6–8]. By these modifications, $LiFePO_4$ cathode has been demonstrated to possess good cycle stability at room temperature.

Electrochemical properties of the $LiFePO_4$-based Li-ion secondary batteries at elevated temperatures are foreseen to be important for electric-vehicles applications. Amine et al. [9] revealed that, while the $LiFePO_4$/mesocarbon microbead (MCMB) cell was cycled with essentially no capacity fading up to 100 cycles at room temperature, the cells cycled at 37 and 55 °C showed significant fading. The accelerated fading at the high temperatures was attributed to the dissolution of Fe from the cathode ($LiFePO_4$) side and subsequent deposition of the Fe ions on the MCMB anode, where the metal deposit catalyzed the formation of the solid/electrolyte interphase (SEI) layer. The formation of the SEI layer consumes Li ions and imposes high surface resistance. Both lead to capacity fading.

Metal oxide coating has often been used to improve the performance of cathode materials [10–20]. Researchers have reported that these oxides, such as Al_2O_3, ZrO_2, MgO, ZnO, and TiO_2, can give multi-functional improvements in cycle performance by, for example, preventing direct contact between the cathode material and the electrolyte, improving the structural stability and so on. However, to our knowledge, similar approach has not yet been tested on $LiFePO_4$.

In this work, TiO_2 was coated onto the surface of $LiFePO_4$ particles by a sol–gel process, and the effects of the oxide coating on the high-temperature (55 °C) cycle performance of the $LiFePO_4$-based cells were studied. The coated $LiFePO_4$ was cycled against either a Li or a C (MCMB) anode. It is demonstrated that, while the employment of the oxide coating indeed reduces capacity fading of

* Corresponding author. Tel.: +886 2 23627158; fax: +886 2 23623040.
E-mail address: nlw001@ntu.edu.tw (N.-L. Wu).

0378-7753/$ – see front matter © 2008 Elsevier B.V. All rights reserved.
doi:10.1016/j.jpowsour.2008.07.021

the $LiFePO_4$/Li cell, it imposes an opposite effect on the $LiFePO_4$/C one. The causes to such improvement and deterioration have been investigated.

2. Experimental

The $LiFePO_4$ powder (Phostech Lithium Inc.) employed has an average particle size of ~5.0 μm and a carbon content of 1.9% by weight. Surface coating of TiO_2 on the $LiFePO_4$ powder was conducted as follows. Firstly, $Ti(C_3H_7O)_4$ (Aldrich, 97%) in ethanol was mixed with the $LiFePO_4$ powder in a molar ratio of $Ti(C_3H_7O)_4$:$LiFePO_4$ = 0.03:1, and the slurry was heated to ~70 °C in ambient until totally dried. The as-prepared powder was then fired in a horizontal oven at 750 °C for 0.5 h under 1% H_2/N_2 atmosphere. X-ray diffraction (XRD) was carried out on a Philip X'pert diffractometer with Cu Kα radiation.

For electrochemical tests, the $LiFePO_4$ electrode contains on a dry basis 86% the $LiFePO_4$ powder either with or without TiO_2 coating, 5% graphitic flakes (KS6, Timcal), 1% nano-sized carbon black (Super P, Timcal), and 8% poly(vinylidene fluoride) (PVdF, Solvay Singapore Pte. Ltd.). Al foil is used as the current collector, and the thickness of the $LiFePO_4$ overlay is ~55 μm. In the $LiFePO_4$/Li cell, a Li foil was used as the counter-electrode; while in the $LiFePO_4$/C cell, a C electrode was used. The C electrode contains 93% MCMB (Osaka Gas) and 7% PVdF. The electrolyte is 1 M $LiPF_6$ in a mixture of ethylene carbonate (EC) and ethyl methyl carbonate (EMC) with a volume ratio of 1:2. The electrodes were assembled into CR2032 coin cells for testing. The cells were cycled at 1C-rate between 2.5 and 4.3 V for the $LiFePO_4$/Li cells and between 2.5 and 3.65 V for the $LiFePO_4$/C cells at 55 °C with a charge-discharge tester (Arbin, model: MCN6410). Cyclic voltammetry (CV) analysis was performed at 5 mV min^{-1}. Both the CV and electrochemical impedance spectroscopy (EIS) measurements were obtained using AUTOLAB, Eco Chenie PSGTAT30.

To prepare samples for surface analyses, the cycled coin cells were dissembled in a glove box under Ar atmosphere, and the electrodes were rinsed with diethyl carbonate (DEC) and dried and stored in the glove box before analysis. Surface and particle morphology were examined by scanning electron microscopy (SEM; LEO1530 and JOEL JSM-6700F). Energy dispersive X-ray spectroscopy (EDS, Oxford Instrument, model: 6587) and X-ray photoelectron spectroscopy (XPS, VG MICROTECH, MT-500) were used to analyze the surface compositions of electrodes.

In one experiment, Fe and Ti films were, respectively, deposited onto different C electrodes, and the deposited C anodes were then cycled against $LiFePO_4$ cathode in order to evaluate the effects of the metal deposit on capacity fading rate. The metal films were deposited by vacuum sputtering under an atmosphere of 5 mtorr Ar with the power condition of 60 mA and 280 V and designated deposition periods that produce films of ~40 nm thick.

3. Results and discussion

For brevity, the TiO_2-coated $LiFePO_4$ powder will hereafter be abbreviated as c-LFPO, while the un-coated powder as u-LFPO. Fig. 1 compares the XRD patterns of the u- and c-LFPO powders. For both patterns, only $LiFePO_4$ was detected. The olivine phase in these two patters show essentially the same lattice constants ($a = 1.025 \pm 0.001$ nm, $b = 0.597 \pm 0.001$ nm and $c = 0.466 \pm 0.001$ nm), suggesting absence of solid solution, which would otherwise cause change in lattice constants. Being inaccessible to direct observation of the TiO_2/$LiFePO_4$ interface by, for instance, high-resolution transmission electron microscopy, the presence of the TiO_2 coating was ascertained by the following analyses. Firstly, a c-LFPO/Li cell was subjected to CV test between

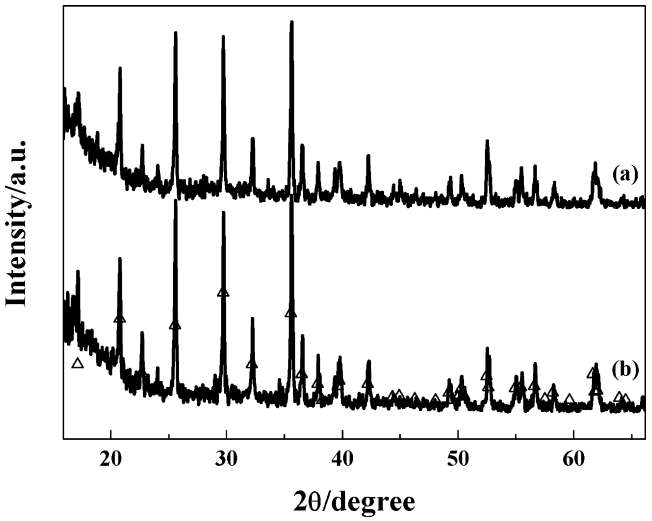

Fig. 1. XRD patterns of (a) pristine and (b) TiO_2-coated $LiFePO_4$. Symbol Δ locates the XRD-peak positions for $LiFePO_4$.

1.0 and 4.3 V. As shown in Fig. 2, in addition to the lithiation/de-lithiation pair of $LiFePO_4$ centered at 3.44 V, there is an additional redox pair centered at 1.84 V. This low-voltage redox pair can be attributed to lithiation/de-lithiation of anatase TiO_2 [21]. Indeed, all the strong reflections of the anatase phase overlapped with the reflections of $LiFePO_4$, and this explains why its presence has not been detected by XRD. Secondly, as shown in Fig. 3a and b, EDS mapping of Ti on individual c-LFPO particles gives fairly uniform Ti distribution. These combined results give unequivocal evidence to the presence of anatase TiO_2 coating on the $LiFePO_4$ particles. Unfortunately the thickness of the coating cannot be determined.

Discharge capacity data for the $LiFePO_4$/Li cells were summarized in Fig. 4. The c-LFPO/Li cell showed a maximum capacity of 145 mAh g^{-1}, and the capacity faded gradually with continuous cycling, retaining 140 mAh g^{-1} after 90 cycles. The u-LFPO/Li cell also exhibited a maximum capacity of 145 mAh g^{-1} but its capacity faded faster, to 132 mAh g^{-1} in totally 90 cycles (open symbols in Fig. 4). The beneficial effect of the TiO_2-coating in reducing capacity fading of the $LiFePO_4$/Li type of cells is clear. Fig. 5 compares the discharge potential curves of the maximum-capacity cycles for the two cells. The curves match perfectly with each other. The coat-

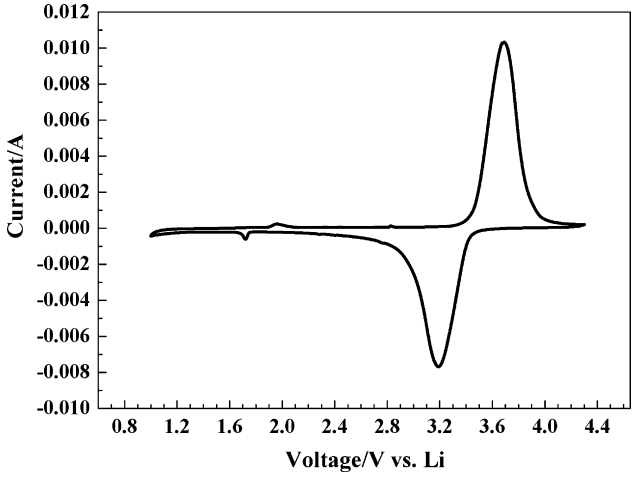

Fig. 2. Cyclic voltammogram of a c-LFPO/Li cell, which contains TiO_2-coated $LiFePO_4$ cathode.

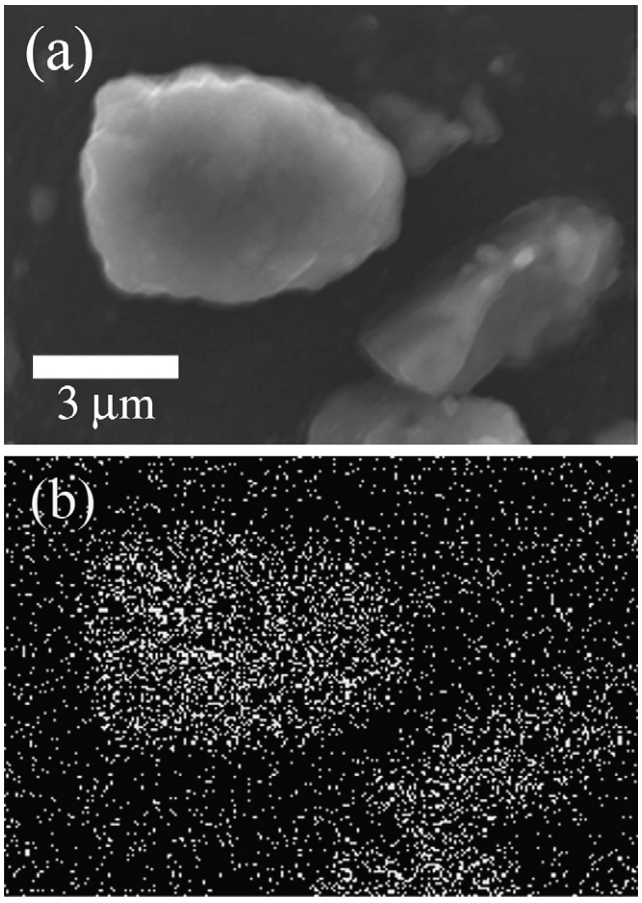

Fig. 3. (a) SEM micrograph of a TiO_2-coated $LiFePO_4$; and (b) the corresponding EDS mapping of Ti.

ing appears having no effect on the fundamental nature of the lithiation/de-lithiation chemistry of $LiFePO_4$.

Fig. 6 compares the EIS profiles of these two cells at selected cycles. All the EIS measurements were carried out at the lower terminal voltage, 2.5 V, i.e., at the fully discharged state, at room temperature. The curves show basically the same characteristics, including a depressed semi-circle within the high-to-middle frequency range and an inclined line within the low frequency range. The curve profile is typical of the electrochemical reaction associated with Li-ion intercalation. The resistance of the semi-circle can be considered as the total interfacial resistance that is equal to

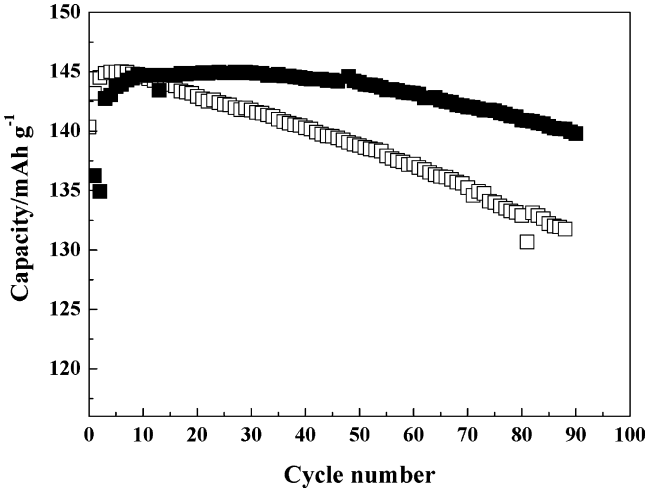

Fig. 4. Specific capacity versus cycle number (■: c-LFPO/Li; □: u-LFPO/Li). The cells were cycled at 55 °C at 1C–1C rate between 2.5 and 4.3 V.

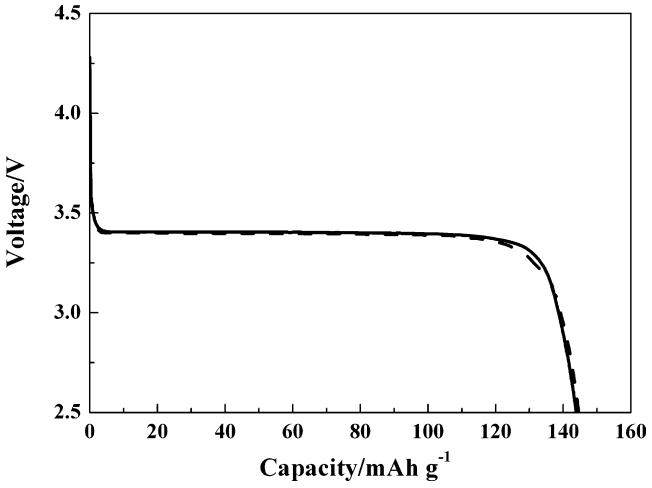

Fig. 5. Comparison of discharge potential curves of the maximum-capacity cycles (solid line: c-LFPO/Li; dashed line: u-LFPO/Li).

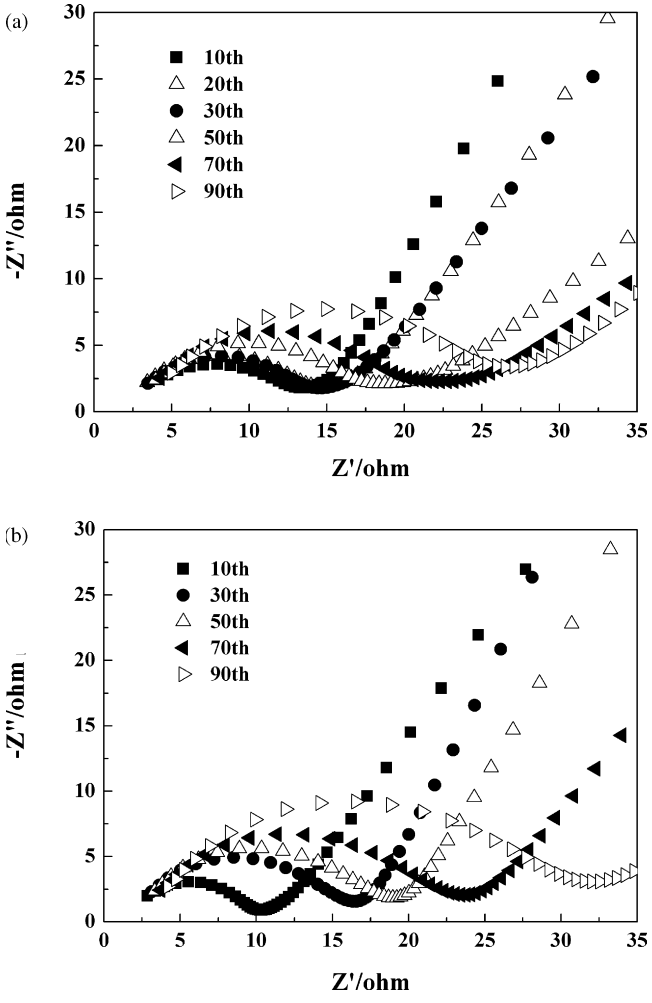

Fig. 6. Nyquist plots of the cells discharged to 2.5 V after selected cycles for (a) the c-LFPO/Li cell and (b) u-LFPO/Li.

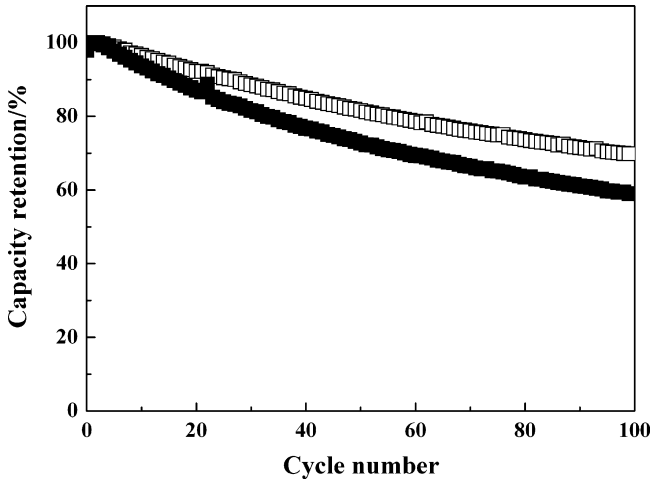

Fig. 7. Capacity retention of the $LiFePO_4$/C type of cells versus cycle number (■: c-LFPO/C; □: u-LFPO/C).

the sum of the resistance of Li^+ migration through the SEI film and the resistance of charge transfer at the solid-film interface [see, for instance, Ref. #22]. This attribution holds for $LiFePO_4$ electrode at the fully discharged or charged state, which falls within the two terminal solid-solution regions of $LiFePO_4$-$FePO_4$ phase diagram [23,24]. As shown in Fig. 6, the interfacial resistance of the u-LFPO/Li cell, 7.0 Ω, is initially lower than that, ~10 Ω, of the c-LFPO/Li cell. However, the former increases more rapidly with cycle number than the latter. After 90 cycles, the u-LFPO/Li cell shows an interfacial resistance of 32 Ω, while the c-LFPO/Li cell 26 Ω. The trend shown by the interfacial resistance coincides with the capacity data. That is, as the interfacial resistance of the u-LFPO/Li cell increases faster with cycling, the cell also exhibits faster capacity fading.

The TiO_2-coating on $LiFePO_4$ particles, however, was found to have an opposite effect on the cycle performance of the $LiFePO_4$/C type of cells, including u-LFPO/C and c-LFPO/C, as show in Fig. 7. When cycled between 3.65 and 2.5 V, both cells exhibited initial maximum discharge capacities near 1.0 mAh, suggesting that they have similar initial properties. Two features are worth noting upon prolonged cycling. Firstly, for both cells, the capacity fades at a faster pace than their $LiFePO_4$/Li counterparts. For instance, the u-LFPO/C cell lost 29% capacity after 90 cycles, while the u-LFPO/Li cell lost only 9.7% (Fig. 4a). The difference is even more dramatic for the TiO_2-coated $LiFePO_4$ electrode; the c-LFPO/C cell lost 39%, in contrast to 3.5% for the u-LFPO/Li. Secondly, for the $LiFePO_4$/C configuration, the u-LFPO/C cell shows a slower fading rate than the c-LFPO/C cell. This is opposite to the trend shown by the $LiFePO_4$/Li cells.

SEM study on the cycled C anodes of both the u- and c-LFPO/C cells showed that the surfaces of the anodes were found to be covered with nodules of SEI materials (Fig. 8a and b). There is apparently a much greater amount of the nodules for the c-LFPO/C cell. EDS analysis of the nodules showed strong F signal. Fig. 9a–d compares the XPS patterns of selected elements acquired from these two anodes. While they give similar intensities of the C and O peaks (Fig. 9a and b), the anode of the c-LFPO/C cell shows distinctly higher intensities of the F and P peaks (Fig. 9c and d). The F peak has a binding energy (b and e) characteristic of LiF [25], suggesting that a greater amount of LiF is deposited on the C anode of the TiO_2-coated $LiFePO_4$ cell. This is consistent with the SEM and EDS results described above, which showed a greater amount of F-rich nodules formed on the surface of the C anode of the c-LFPO/C cell.

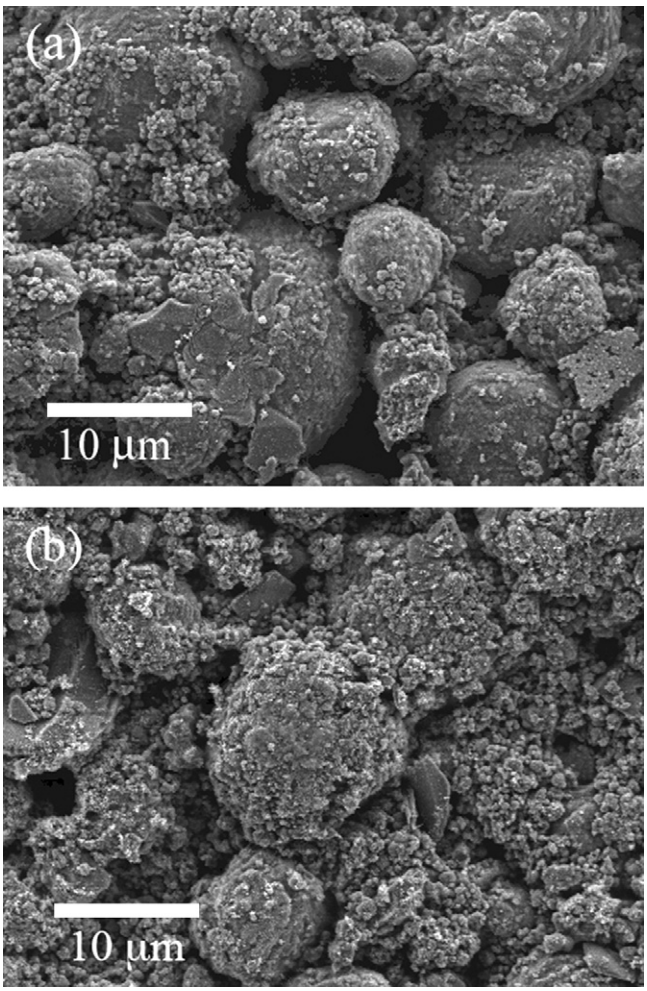

Fig. 8. SEM micrographs of the C anodes from (a) u-LFPO/C and (b) c-LFPO/C.

XPS analysis detected Fe signal on both anodes. Fig. 10 plots the Fe XPS signal intensity as a function of sputtering depth. The data confirmed the occurrence of Fe deposition on both C anodes. Furthermore, it is shown that there is less amount of Fe deposited on the C anode of the c-LFPO/C cell than on the anode of the u-LFPO/C cell. On the other hand, the former additionally showed Ti signal but the latter did not (Fig. 11). The Ti appearing on the C anode of the c-LFPO/C cell must have come from the TiO_2 coating on the cathode side. The results indicate that Ti ions were dissolved from the cathode side and subsequently reduced on the C anode in the c-LFPO/C cell during the cycling process. Possible dissolution of Ti ions has not been addressed in the earlier studies concerning the TiO_2-coated cathodes [17–20].

The capacity data of the $LiFePO_4$/Li cells in Fig. 4 have demonstrated reduced capacity fading rate as a result of the TiO_2-coating on the $LiFePO_4$ powder. This is in agreement with the general trend that has been reported in several other TiO_2-coated cathode materials, such as $LiCoO_2$ [17,18], $LiMn_2O_4$ [18,19], and $LiNi_{1/3}Mn_{1/3}Co_{1/3}O_2$ [20]. In all these studies, the TiO_2-coated cathodes have been cycled against Li metal electrode. Taking into account all the analysis results presented above, we infer that the fading improvement is largely because the presence of the TiO_2 coating helps to prevent direct contact between the $LiFePO_4$ particles and the electrolyte, and hence it reduces erosion of $LiFePO_4$ upon cycling. As pointed out by Amatucci et al. [26] in their study on $LiMn_2O_4$, dissolution of metal ions may lead to the formation

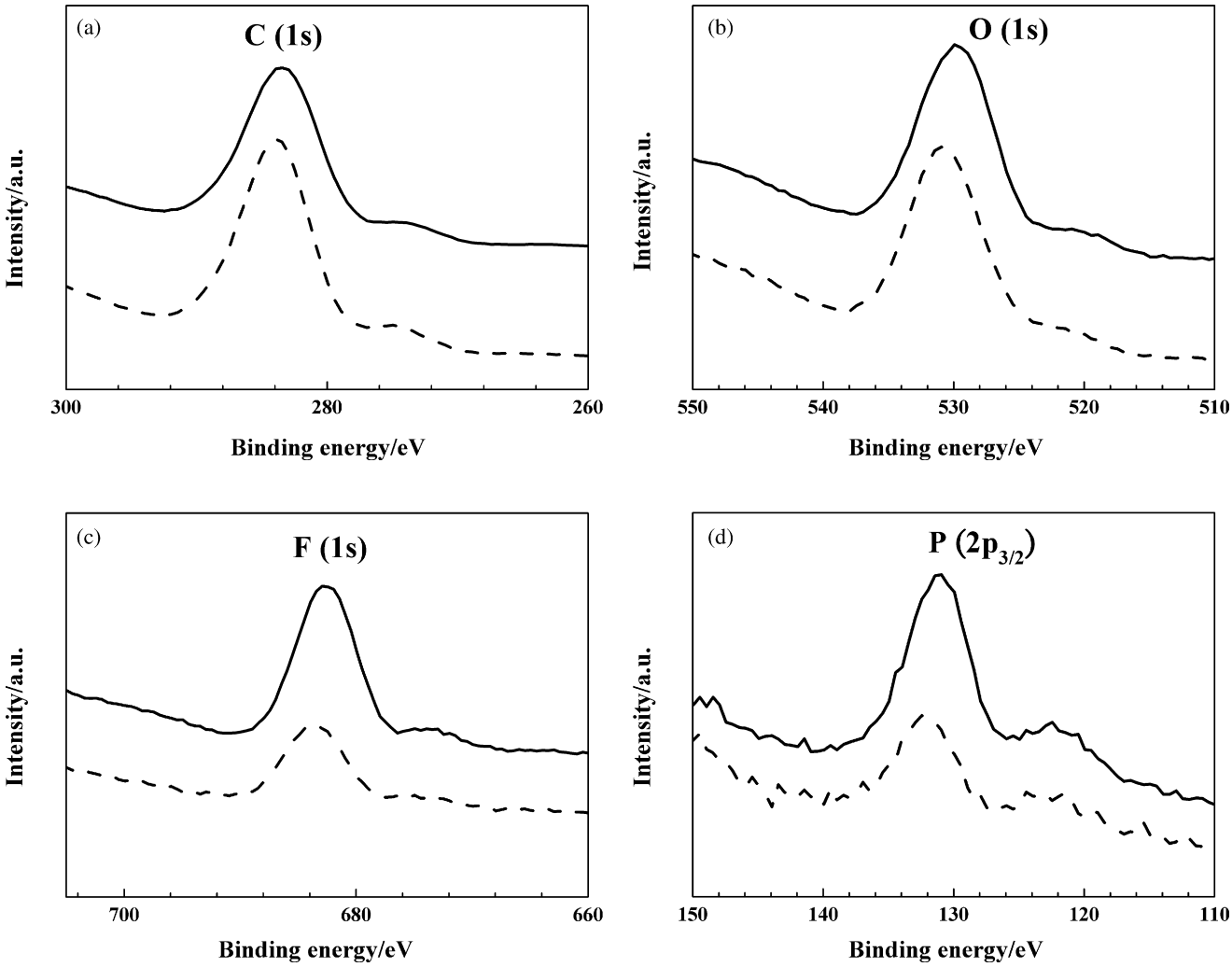

Fig. 9. XPS spectra of (a) C (1s), (b) O (1s), (c) F (1s), and (d) P ($2p_{3/2}$) acquired from the surface of the C anode of (solid line): c-LFPO/C; and (dashed line): u-LFPO/C.

of passivating surface layer of high charge-resistance on cathode, which, along with material loss, contributes to capacity fading. This is consistent with the observation that the c-LFPO/Li cell has a lower increasing rate in interfacial resistance than the u-LFPO/Li cell upon cycling (Fig. 6). Furthermore, the XPS data (Fig. 9) also confirmed that, in the case of the $LiFePO_4$/C type of cells, there is less Fe deposition on the C anode cycled against c-LFPO than against u-LFPO.

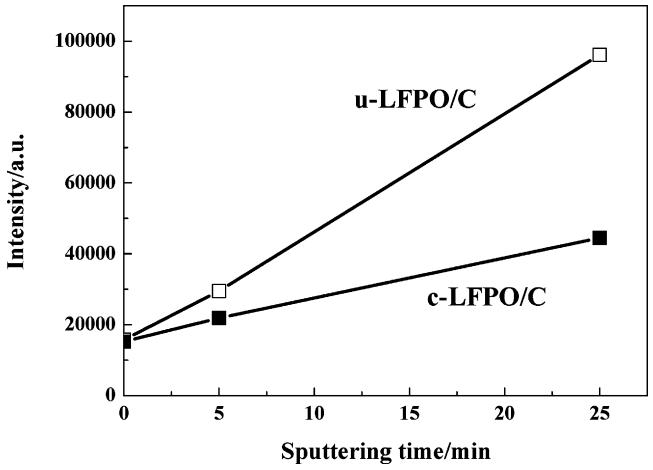

Fig. 10. Fe XPS signal intensity from the C anode as a function of sputtering time (■: c-LFPO/C; □: u-LFPO/C).

The $LiFePO_4$/C type of cells exhibited a completely opposite trend in cycling stability to the $LiFePO_4$/Li cells. That is, the c-LFPO/C cell showed a faster capacity fading rate than the u-LFPO/C cell (Fig. 7). Different from the $LiFePO_4$/Li cells, the $LiFePO_4$/C cells have only limited amount of Li ions. As the SEI formation consumes Li, the cell that exhibits more SEI materials formation is expected to show a faster capacity fading. This is consistent with the SEM and XPS results (Figs. 8 and 9), which show that there has indeed been more SEI formation on the C anode of the c-LFPO/C cell. The question is now why the cell, c-LFPO/C, showing less Fe deposition at anode turns out to have a greater amount of SEI materials.

As shown by XPS, in addition to Fe, there was also Ti deposition on the C anode of the c-LFPO/C cell. The effect of Ti deposit on the cycling performance of the olivine cathode has never been determined in the literature. To evaluate such effects, the following experiment was conducted. Ti and Fe layers were, respectively, deposited onto different C electrodes by vacuum deposition, and the electrodes were then cycled against u-LFPO cathode. Fig. 12 compares the capacity data between these two cells. Data of the cell without any pre-deposited metal film are also shown. It was found that the cell containing the Ti-coated anode shows the fastest

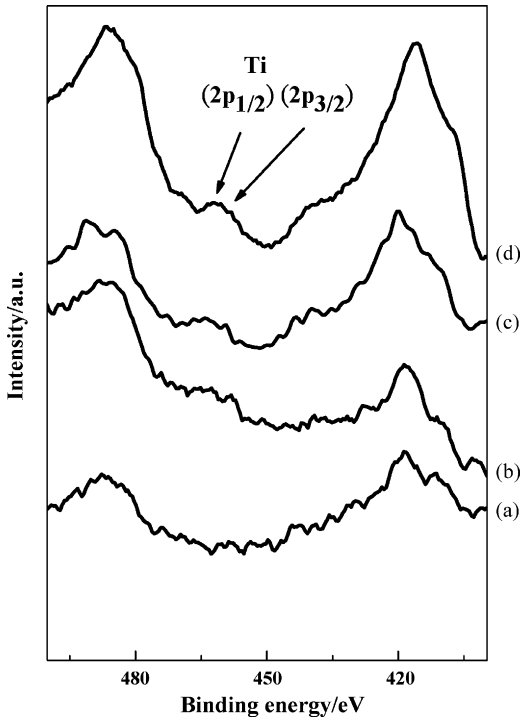

Fig. 11. XPS spectra of Ti from the MCMB anode of (a) u-LFPO/C and (b–d) c-LFPO/C with different sputtering times: (b) 0, (c) 5, and (d) 25 min.

capacity fading than the rest cells. As shown by SEM analysis (Fig. 13), the SEI layer on the Ti-coated C anode is very thick, showing uniformly covered film morphology. On the other hand, the granular nature of the MCMB particles can still be seen on the Fe-coated anode. The pre-deposited Ti layer apparently has a much greater catalytic activity in accelerating SEI formation than the Fe layer. Therefore, one may anticipate that Ti deposited on the C anode causes more pronounced deteriorating effect on capacity performance than the Fe deposit. This result explains why the c-LFPO/C cell, which shows Ti deposition on the C anode, exhibits faster capacity fading than the u-LFPO/C cell.

It is worth noting that large majority of the past studies concerning metal-oxide coating on cathodes have been using Li as the counter electrode. The results of the present study point out the need to re-evaluate those coating materials for their chemical stability under cycling as well as for their potential deteriorating effect on the anode side.

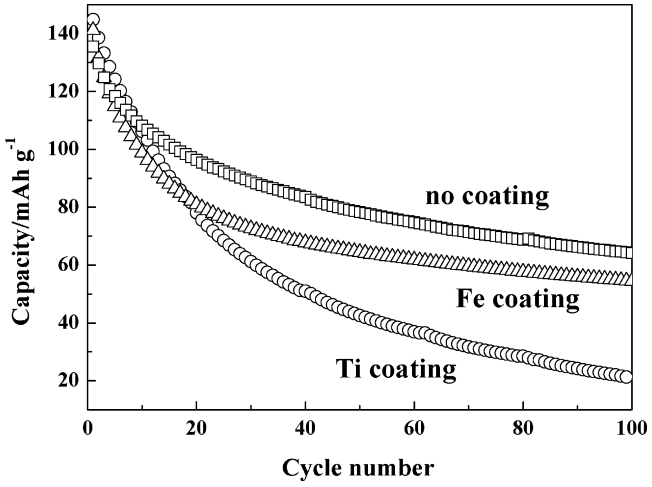

Fig. 12. Discharge capacity versus cycle number for the u-LFPO/C cells of which the C anode is coated with (Δ) Fe layer, (○) Ti layer, and (□) no metal layer.

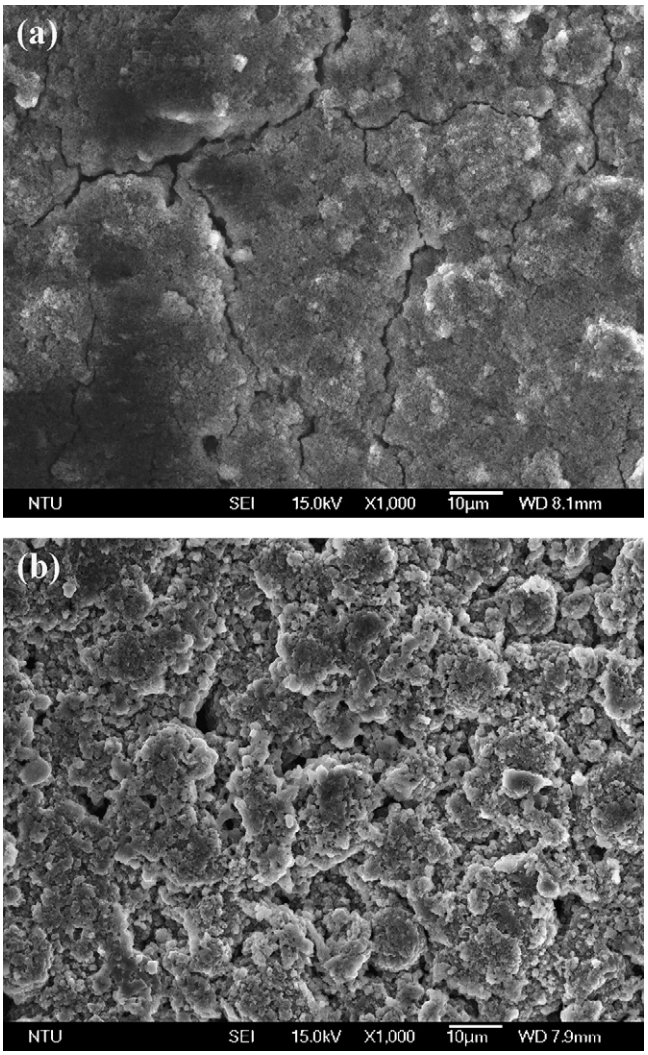

Fig. 13. SEM micrographs of the C anodes of the u-LFPO/C cells of which the anodes are initially coated with a layer of (a) Ti and (b) Fe.

4. Conclusions

The effects of TiO_2 coating on the cycling performance at 55 °C of the $LiFePO_4$ cathode against either a Li or a C anode have been studied. It has been demonstrated that, while the presence of the oxide coating helps to reduce capacity fading for the $LiFePO_4$/Li cell, it imposes an adverse effect on the $LiFePO_4$/C cell. The analysis results indicate that the presence of the TiO_2 coating helps to reduce the Fe dissolution problem at the cathode. However, the coating itself is not stable and partially dissolved upon cycling, causing re-deposition of Ti at the C anode. Ti deposit has been shown to be more active than Fe in causing SEI layer formation at the anode, leading to accelerated capacity fading.

Acknowledgments

This work was partly supported by the National Taiwan University (NTU) under contract number of 95R0066-BE04-01 and by the Material and Chemical Research Laboratories, Industrial Technol-

ogy Research Institute, Hsinchu, Taiwan. The authors thank Prof. M.-T. Lin and Mr. K.-S. Li at the Department of Physics, NTU, for their assistance on thin-film deposition.

References

[1] A.A.M. Prince, S. Mylswamy, T.S. Chan, R.S. Liu, B. Hannoyer, M. Jean, C.H. Shen, S.M. Huang, J.F. Lee, G.X. Wang, Solid State Commun. 132 (2004) 455.
[2] A.K. Padhi, K.S. Nanjundaswamy, J.B. Goodenough, J. Electrochem. Soc. 144 (4) (1997) 1188.
[3] N. Ravet, Y. Chouinard, J.F. Magnan, S. Besner, M. Gauthier, M. Armand, J. Power Sources 97–98 (2001) 503.
[4] P.P. Prosini, D. Zane, M. Pasquali, Electrochim. Acta 46 (2001) 3517.
[5] H.C. Shin, W.I. Cho, H. Jang, Electrochim. Acta 52 (2006) 1472.
[6] S.-Y. Chung, J.T. Bloking, Y.-M. Chiang, Nat. Mater. 1 (2002) 123.
[7] H. Xie, Z. Zhou, Electrochim. Acta 51 (2006) 2063.
[8] D. Wang, H. Li, S. Shi, X. Huang, L. Chen, Electrochim. Acta 50 (2005) 2955.
[9] K. Amine, J. Liu, I. Belharouak, Electrochem. Commun. 7 (2005) 669.
[10] T. Fang, J.-G. Duh, S.-R. Sheen, Thin Solid Films 469–470 (2004) 361.
[11] J. Cho, T.-G. Kim, C. Kim, J.-G. Lee, Y.-W. Kim, B. Park, J. Power Sources 146 (2005) 58.
[12] Y.-J. Kim, J. Cho, T.-J. Kim, B. Park, J. Electrochem. Soc. 150 (2003) A1723.
[13] K.Y. Chung, W.-S. Yoon, J. McBreen, X.-Q. Yang, S.H. Oh, H.C. Shin, W.I. Cho, B.W. Cho, J. Electrochem. Soc. 153 (2006) A2152.
[14] H.L. Zhao, L. Gao, W.H. Qiu, X.H. Zhang, J. Power Sources 132 (2004) 195.
[15] Y. Iriyama, H. Kurita, I. Yamada, T. Abe, Z. Ogumi, J. Power Sources 137 (2004) 111.
[16] H.S. Liu, Z.R. Zhang, Z.L. Gong, Y. Yang, Solid State Ionics 166 (2004) 317.
[17] A.M. Kannan, L. Rabenberg, A. Manthiram, Electrochem. Solid-State Lett. 6 (2003) A16.
[18] Z.R. Zhang, Z.L. Gong, Y. Yamg, J. Phys. Chem. B 108 (2004) 17546.
[19] L.H. Yu, X.P. Qiu, J.Y. Xi, W.T. Zhu, L.Q. Chen, Electrochim. Acta 51 (2006) 6406.
[20] D.C. Li, Y. Kato, K. Kobayakawa, H. Noguchi, Y. Sato, J. Power Sources 160 (2006) 1342.
[21] L. Kavan, M. Kalbác, M. Zukalová, I. Exnar, V. Lorenzen, R. Nesper, M. Graetzel, Chem. Mater. 16 (2004) 477.
[22] G. Sikha, R.E. White, J. Electrochem. Soc. 154 (2007) A43.
[23] V. Srimivasan, J. Newman, J. Electrochem. Soc. 151 (2004) A1517.
[24] A. Yamada, H. Koizumi, N. Sonoyama, R. Kanno, Electrochem. Solid-State Lett. 8 (2005) A409.
[25] J.F. Moulder, W.F. Stickle, P.E. Sobol, K.D. Bomben, in: J. Chastain, R.C. King Jr. (Eds.), Handbook of X-ray Photoelectron Spectroscopy, Physical Electronics, Eden Prairie, MN, 1995, p. 35.
[26] G. Amatucci, A. Du Pasquier, A. Blyr, T. Zheng, J.M. Tarascon, Electrochim. Acta 45 (1999) 255.